Energy Equip. Sys./ Vol. 5/No . 3/September 2017/ 251-264

ENERGY EQUIPSYS

Energy Equipment and Systems

http://energyequipsys.ut.ac.ir
www.energyequipsys.com

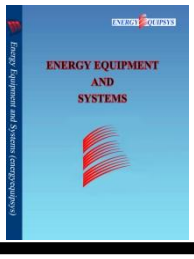

An investigation on effect of backbone geometric anisotropy on the performance of infiltrated SOFC electrodes

Authors

Mehdi Tafazoli [a]
Mohsen Shakeri [a*]
Majid Baniassadi [b]
Alireza Babaei [c]

[a] Mechanical Engineering Department, Babol Noshirvani University of Technology, Babol, Iran

[b] School of Mechanical Engineering, College of Engineering, University of Tehran,Tehran, Iran

[c] School of Metallurgy and Materials Engineering, College of Engineering, University of Tehran, Iran

ABSTRACT

Design of optimal microstructures for infiltrated solid oxide fuel cell (SOFC) electrodes is a complicated process because of the multitude of the electrochemical and physical phenomena taking place in the electrodes in different temperatures, current densities and reactant flow rates. In this study, a stochastic geometric modeling method is used to create a range of digitally realized infiltrated SOFC electrode microstructures to extract their geometry-related electrochemical and physical properties. Triple Phase Boundary (TPB), active surface density of particles along with the gas transport factor is evaluated in those realized models to adapt for various infiltration strategies. Recently, additive manufacturing or freeze type casting methods enable researchers to investigate the performance of directional electrodes to get the maximum electrochemical reaction sites, gas diffusivity and ionic conductivity simultaneously. A series of directional backbones with different amount of virtually deposited electrocatalyst particles are characterized in the first step. The database of microstructural parameters (inputs) and effective geometric properties (outputs) is used to train a range neural network. A microstructure property hull is created using the best neural network model to discover the range of effective properties, their relative behaviour and optimum microstructure. The characteristics of models is shown that there is not any contradiction between the high level of TPB and contact surface density of particles, but the highest amount of gas diffusivity can be found in the microstructures with lower level of reaction sites. Also increasing the contact surface density has a negative effect on gas transport but the high level of TPB density is feasible in the full range of microstructures. In the other hand, TPB density and gas diffusion into the models are inversely related, although there are a limited number of microstructures with high level of reaction sites and acceptable gas diffusivity. Finally, using a simple optimization process, the microstructures with the highest level of reaction sites and gas transport factor are identified which have the backbone porosity of about 50%, and extremely higher gain growth rate normal to the electrolyte. Additive manufacturing and 3D printing methods will enhance researchers in the future to create the real directional electrodes on the base of these proposed models.

Article history:

Received : 14 February 2017
Accepted : 2 May 2017

Keywords: Backbone Anisotropy, Infiltrated Electrode, Realization of Microstructure, Solid Oxide Fuel Cells.

1. Introduction

Fuel cells as one of the sustainable and environment-friendly energy conversion devices have received interest and generated considerable expectations over the last few decades[1],[2]. SOFCs represent one of the most efficient high temperature fuel cell with capability of direct conversion of fuels into electricity with minimal environmental impact [3].The significance of microstructure in solid oxide fuel cells has been clearly appreciated. Pore size, pore volume fraction, TPB and tortuosity are considered as the most crucial microstructural parameters that greatly affect the electrochemical performance of SOFCs [4],[6] and it should be understood to develop optimum electrodes with higher performance [6]. Recent development of more sophisticated microstructural characterization tools has now enabled researchers to explore microstructure of SOFC by investigating the complex interplay between gas and solid phases and their relationship to performance [7]. Direct imaging of three-dimensional SOFC electrode microstructure with focused ion beam scanning electron microscopy (FIB-SEM) and X-ray computed tomography (XCT) are now used to obtain more quantitative measures such as TPB length and tortuosity factor [8].

Infiltrated electrodes, which are made of a backbone with impregnated particles, are keys for the enhancement of fuel cell performance because of the easier control of composition and particle sizes. A summary of the history and the latest developments in infiltration techniques for this application can be found in [9, 10].

The traditional porous electrode microstructures have been investigated extensively but such morphologies are not ideal for gas diffusion because of the high tortuosity factor, consequently limiting SOFC cell performance. Hence, Those pore structure was modified by changing the morphology or packing of the pore formers [11], [12] using new fabrication method like freeze-drying tape-casting to form hierarchically oriented channels/pores in the SOFC electrodes [13-16]. For instance, Sofie et al. have fabricated a functionally graded and continuously aligned pore structures by a modified tape-casting process for use as solid oxide fuel cell electrodes, catalysts, sensors[17]. Chen et al. in another work have developed a novel functionally graded and acicular Ni-YSZ[1] anode with YSZ as the electrolyte to enhance the electrochemical performance of the cell [15, 18]. Recently they extended their research by determining the porosity distribution and tortuosity factor of these hierarchically oriented microstructures via 3D X-ray microscopy[16]. Their three dimensional hierarchically porous SSC–GDC cathode networks with fine SSC particles showed the highest cell power output ever achieved with the same cell materials [19]. They also presented an innovative design for enhancing the coking resistance of the conventional SOFC anode. They deposited uniformly a SDC[2] catalyst layer on the wall surface of the Ni–YSZ as YSZ internal gas diffusion channel by freeze-drying tape-casted anode via infiltration. The efficiency for catalyst infiltration has been significantly improved by using hierarchically porous anode structure with open and straight channels. [20]. Also, Torabi et al. investigated the impact of porous support morphology on the electrochemical performance of LSM-infiltrated symmetrical cells. They qualitatively analyzed the influence of size, connectivity and distribution of the pores as well as the configuration of YSZ particles on the surface area and three-phase boundary length by scanning electron microscopy [21]. Cassidy et al. have some porous structures with controlled porosity in terms of size and morphology to find the link between the morphology of porous scaffolds and the infiltrated catalyst and understanding these complex relationships to design optimized porous infiltrated structures in the future [22].

In addition to the recent progress in micro/nano imaging and characterization methods, advanced computational techniques were also developed to predict the effects of microstructure geometry on the physical and electrochemical properties of electrodes. For instance, Zhang et al. [23] developed a model to construct a 3D microstructure of infiltrated SOFC electrodes by randomly generating

*Corresponding author: Mohsen Shakeri
Address: Mechanical Engineering Department, Babol Noshirvani University of Technology, Babol, Iran
E-mail address: shakeri@nit.ac.ir

[1] Ni–yttria-stabilized zirconia
[2] Samaria doped ceria

particles on the surface of virtual backbones. They have reported the geometric properties of the electrode, including the percolation threshold of infiltrated nanoparticles and pores, TPB length, nanoparticles surface area, backbone surface area and interfacial area between the backbone and nanoparticles. Zhang et al. [24] have developed a model for the dual-phase infiltration procedure. Bertei et al. [25] have developed a numerically reconstructed model for infiltrated electrodes by employing a sedimentation algorithm for the backbone generation and a novel Monte-Carlo packing algorithm for the random infiltration. Their study shows that the electrodes made by infiltration may show up to two orders of magnitude increase in TPB density compared to conventional composite electrodes. Synodis et al. [26] have presented a mechanistic model to predict both the percolation threshold and effective conductivity of the infiltrated SOFC electrodes. Hardjo et al. [27] presented a methodology to relate an experimentally observed degradation in the effective electronic conductivity of infiltrated electrodes to a reduction in active TPB length as a function of time. A mechanistic model to predict the active TPB density, in combination with effective conductivity of infiltrated SOFC electrodes is presented by Reszka et al. [28]. Recently Kishimoto et al. [6] have conducted a comparison between the nickel-infiltrated gadolinium-doped ceria electrodes and conventional electrodes in regard of TPB density and mean particle/pore sizes to investigate the effect of the microstructural parameters on the effective transport coefficients and electrochemical reaction rate of the electrode [6, 29].

Whereas the process of microstructure simulation of theses complicated electrochemical devices is complicated and time-consuming, a new approach like artificial neural networks (ANNs) is needed to correlate the multi input/output parameters in those models [30-32]. For instance, Marra et al. [33] have used a neural network to estimate the Solid Oxide Fuel Cell performance also bozorgmenhri et al. [34] are employed ANN and a genetic algorithm (GA) to model the effect of constructive parameters (anode porosity, electrolyte thickness, electrode support/functional layer thickness) of a single SOFC power density. The performance of this method is determined by varying error goals, number of neurons, number of layers and training algorithms.

In our previous work [35], the role of backbone geometric anisotropy in infiltrated SOFC electrodes was investigated in another study in 63 different realized microstructures. In that study it was shown that the pore tortuosity changed from 1.2 to 9 depends on the backbone porosity also the TPB and Active surface density of deposited particle was affected by the backbone geometric anisotropy in a manner that the optimum amount of particle loading was changed compared with the traditional electrodes. Additionally the gas transport in directional backbones significantly reduced in high amount of particle loadings on the scaffolds with low porosity. Generally, if the backbone grains are aligned normal to the electrolyte, more electrochemical reaction sites (especially particle surface density) would be available in addition to better gas diffusivity.

In this study, those numerically realization methods in infiltrated microstructures were combined with idea of using hierarchically oriented backbones which are generated by a special statistical method instead on randomly agglomerating spheres. When those virtual models are geometrically characterized, particles were added on the active surface of backbones by a novel algorithm which can control the loading and the aggregation behaviour of particles. Then, these mathematical and 3D-realized microstructure models were characterized to identify the reaction sites and fluid flow properties in different particle loadings and directional behaviour of scaffolds. Then all of those input and output geometric data is used to train a neural network and generating a set of possible microstructures with different effective properties (property hull) which can determine the limitation of microstructure properties and their interactions to correlating the constructive parameters to those properties and generating a powerful search engine in different optimization scenarios. These data can help researchers to find how electrochemical performance affected by geometric properties and provide a way to optimize the infiltration and backbone manufacturing process simultaneously.

2.Scientific Approach

2.1.Microstructure realization and Characterization

To achieve realistic microstructures, in this

study, a series of anisotropic 3D microstructures was generated using Monte-Carlo that is composed of three steps: i) generation, ii) distribution and iii) growth of the cells. First, several initial seed cells are randomly placed in a unit cell of the electrode. Upon initial seed placement, the growth step starts following a cellular automation algorithm. Nucleation rate of primary seeds and growth factor of cells in x- , y- and z-direction also can be controlled. This procedure continues till desired volume fraction for each phase is achieved or all phases meet and fully occupy the grid. Penetration between the phases is avoided at all times throughout the initial distribution and growth of the cells. This code was developed by Baniassadi et al. and completely introduced in ref [36, 37].

One of the most important aspects of the model is the size of representative volume element (RVE) to establish an applicable link between the RVE properties and full electrode model. A number of researchers in [38-40], based on statistical methods, have concluded that the RVE should cover at least 7*7 particles in each side and a particle diameter should be divided at least into 20 voxels to guarantee adequate precision in the evaluation of effective properties. Whereas based on the line intercept, the evaluated particle size of solid phase in this study is in the range of 30 to 10 voxel edge length in the backbone porosity of 25% up to 64%, (the RVE size considered 150×150×150 voxels), it fortunately meet the validation criteria. hence, the average particle diameter of backbone microstructure is in the range of 500-750 nm that is in the normal range of powder grading in SOFC materials also it corresponded to the range of 20-30 nm for the length of voxel edge that would be the minimum size of deposited particles.

When the generation and characterization of the backbone are finished, as discussed in another study, particles would be added into the realized microstructures. In that modelling approach, particles in the form of separate single cubic voxels are aggregated to create a wide variety of geometric shapes on the surface of backbone. In that process, a number of particles are deposited on the active surface of backbone as preliminary seeds completely randomly or as a function of geometric parameters. Depending on the modelling adjustments (Agglomeration and dispersion ratio) the rest of particles are deposited on the surface of pre-deposited seeds or on the backbone surface near to the pre-deposited seeds. Those parameters can be evaluated from high resolution digitized 2D cross section images using image processing software by extraction of geometric properties of assumed skullcaps.

After the realization stage, a wide range of geometric properties are characterized. The most important geometric parameters are determined based on the infiltration strategy which controls the material characteristics of electrode backbone and particles. In this study, it is assumed that the backbone is made of mixed Ionic electric conductor material (MIEC) and highly electrochemically active materials (like Pd, Ru,...) are added to these electrodes to enhance the oxygen reduction on the surface of backbones and alleviate the polarization resistance by increasing the electrochemically active surface density of electrode. [10, 41,43]. In the other word, the density of active TPBs, plays a major role in the overall microstructure of the SOFCs and significantly affects their efficiency [44] also a number of researchers suggested that double phase boundaries between deposited particles and active reactant gas routes can play an important role in electrochemical reactions especially when highly active electrochemical particles are deposited on the surface of MIEC backbones[30, 45]. Hance, active surface density of particles and their triple phase boundary with the scaffold are selected as the electrochemical performance indicators. Also the diffusivity of reactant gas is considered as another rate limiting phenomena especially in high current densities or high temperature working conditions [30].

The TPB density is evaluated by updating the method of Cronin et al [46, 47] with new acceptable neighbourhood patterns in virtual infiltrated microstructures. Then that value is modified with a correction factor (L=10E-4) to correlate our assumptions in the RVE domain size and further normalization process.

In addition to TPB calculation, to extract the contact surface density of particles, all of the active contact situations between different voxelized phases are identified. Then the active surface density of deposited particles is sorted from the identification matrix of realized microstructures.

The Gas transport factor is a function of the porosity and tortuosity of the gas routes based on the modified version of Fick's law for porous media [48]. In this study, the porosity (φ) is evaluated directly from the

identification matrix and the (τ) is obtained from the effective thermal conductivity of realized 3D models of microstructures. The knudsen diffusion is neglected due to the assumed ratio of molecular distance of passing gas and average pore size and the gas transport factor is estimated by this equation:

$$\text{Diffusion factor} = \frac{\varepsilon}{\tau} \quad (1)$$

2.2.Microstructure and property Hull

To design required material and geometry together for a special purpose, a microstructure hull can be used. It is consists of a set of possible microstructures with different materials. Certain distribution functions can correlate it to a property hull containing a region of characterized properties of those microstructures. In the other word, that closure includes all possible effective property values predicted by sweeping input parameters defining these distribution functions. Mathematically speaking, a property closure for those parameters can be obtained using an arbitrary analytical or approximate method and their boundaries represent constraints for the optimization process [49, 50]. As discussed before, TPB density, Contact surface density of particles and gas transport factor are selected as critical design objectives in this study to form the property hull.

3.Methodology

To realize the effect of geometric anisotropy in backbones, the statistical function of growth rate, normal to the electrolyte (Z), is changed to achieve 5 different morphology in 3 level of scaffold porosity (55%,45%,35%). In the first step, the most important geometric properties (Tortuosity, Active surface density and particle/pore size) of realized backbones are completely identified. Then particles in the form of single voxels are added into the scaffold microstructures. The particle volumetric loading is set in the range of 2.5% -15% to provide enough gas diffusivity. 20% of particles are considered as primary seeds and the aggregation ratio is set in a manner that 30% of particles are aggregated only on the pre-deposited particles and the rest are deposited on the surface of backbone and pre-deposited particles or seeds. Five samples of 3D realized models with the backbone porosity of 45% and 5% loading of particles are shown in Fig.1 .The main direction of backbone grains is completely normal to the electrolyte in the left model and gradually it changes parallel to the electrolyte.

Finding the optimal geometric properties in those kinds of infiltrated microstructures is a complicated task; additionally the most effective electrochemical mechanisms in an energy conversion device are determined by the intrinsic property of materials and the working condition of the cell. Linking those geometric parameters and rate limiting electrochemical and physical processes can be done by creating a microstructure and correlated property hull.

The neural network framework could be a solution to predict the properties of the microstructures for a given set of input parameters. Hence, as shown in Fig.2, a number of neural networks are trained to predict the properties of the microstructures for a given set of input parameters. In the current study, the extrapolation in input and output parameters is limited carefully because of the complicated behaviours of fuel cells. A set of back propagation neural networks (BPNN) based on four inputs (backbone porosity, Axial and transversal growth rates and particle loading) and three normalized outputs (TPB Density, Particle contact surface density and gas diffusion factor) are trained using Neural Network Toolbox provided in MATLAB™.

Those models consists of an input layer, one or two hidden layer with up to 30 neurons with tan-sig transfer function and an output

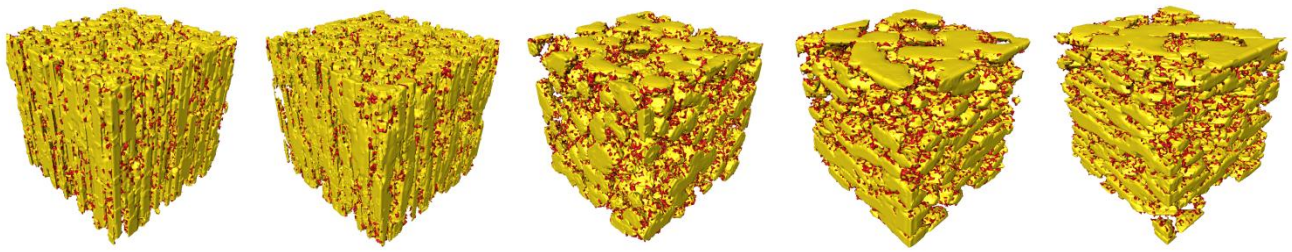

Fig.1.3D-Realized models of virtually infiltrated microstructure with directional backbones

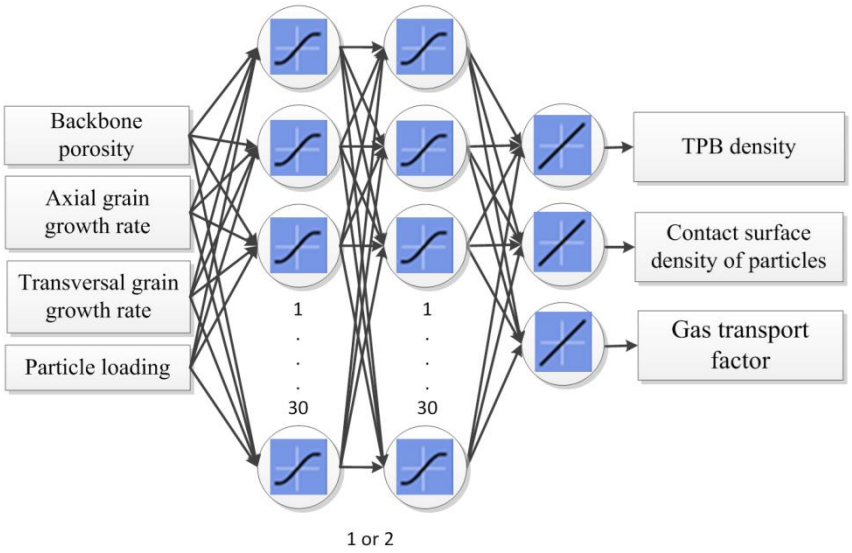

Fig.2. The neural network structure to predict microstructure properties

layer with 3 neurons with linear transfer function. 70 percent of data is dedicated for neural network training and the reminded data is used for testing and validation of the model.

When the best trained neural network is identified, it can be used to properly predict the output parameters in terms of input variables. In the other words, the microstructure hull by sweeping feasible input variables in an acceptable range can be correlated to the property closure using that model. Due to complex electrochemical behaviour of fuel cells the range of input microstructural parameters are not be exceed the previously reported input parameters to avoid improper extrapolation of data. Thus, by enabling the researcher to predict the variation of output parameters in some specific domains, a search engine for further optimization techniques can be provided, as shown in Fig.3.

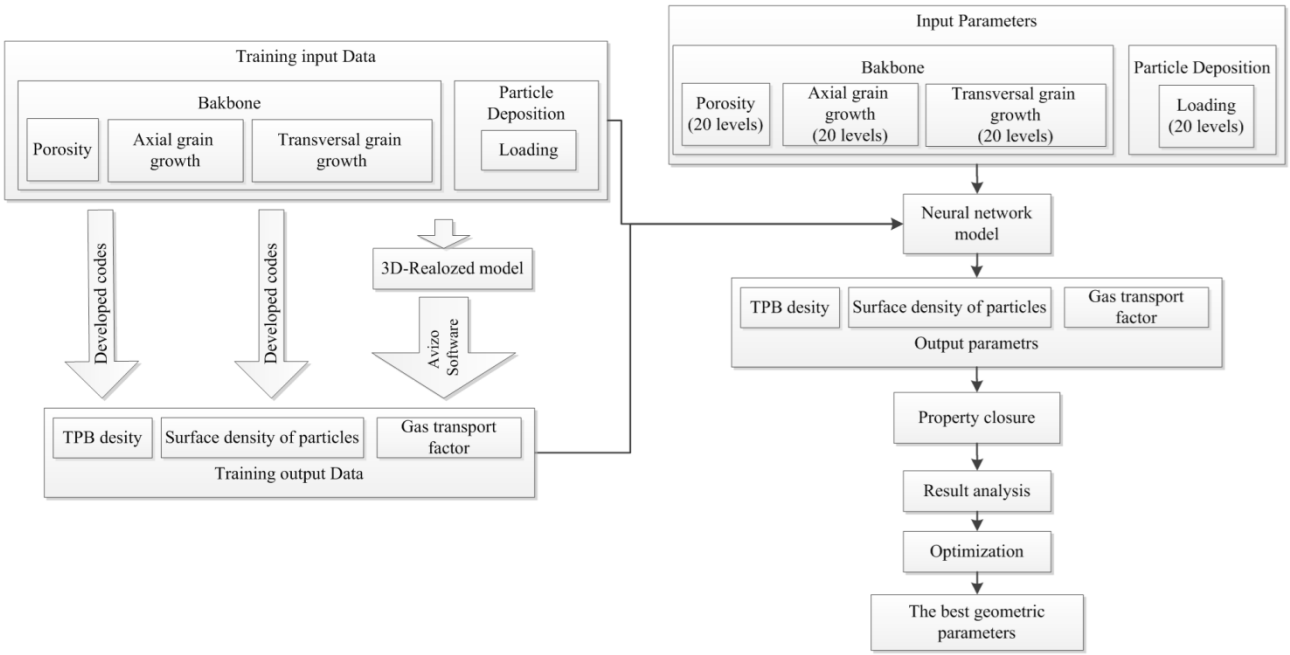

Fig.3.Schematic diagram showing different sections of the study and their relationship

In this study, Porosity, Axial (Z) and transversal (XY) growth rate of backbone grains and volumetric loading of particle are divided into 20 levels in the range of pre-realized microstructures to simulate the overall relationship between the microstructural variables and its geometric properties in microstructure and property hull.

4.Result and discussion

Following these input specifications and their combinations, among the feasible combination of these parameters, 63 different microstructures are realized and then characterized in regard of their properties as shown in Fig.3. TPB density and contact surface densities are evaluated directly from the mathematical model, but the gas diffusion factor is evaluated from the 3D realized models.The range of input and output variables are listed in Table 1.

Those results are used to train different neural network structures. The mean square errors (MSE) of those models are compared in those models to find the best fit model. For example in one hidden layer models as shown in Fig.4, the least MSE is achieved about 1.1167e-05 in a model with 15 neurons in the hidden layer. Also in two layer models, the least MSE is achieved about 1.3506e-06 in a model with 16 neurons in the first hidden layer and 23 neurons in the second layer.

The best trained neural network is used to predict the properties of 160000 hypothetical microstructures based on the process of Fig.3 to create a property hull. Among those models, 33154 microstructures have the acceptable range in outputs (more than zero) as listed in Table 2. Based on the obtained properties, it is clear that the gas transport factor and contact surface density of particles are respectively 1.35 and 1.07 times more sensitive to the geometry than the TPB density with our assumptions.

Those hypothetical microstructures in the form of small points are specified in Fig.5 to form a simple property closure. Each axis represents one of the most important properties of assumed models in the feasible range design space.

Table 1.The range of input and output parameters 63 realized microstructure (training data)

		minimum	maximum	variation
input	porosity volume fraction	0.300	0.533	0.232
	Z growth	0.001	0.999	0.998
	XY growth	0.001	0.999	0.998
	loading	0.025	0.15	0.125
output	TPB density (L μm^{-2})	0.053	0.207	0.154
	contact surface density of particles(L μm^{-1})	0.062	0.296	0.234
	Gas transport factor	0.059	0.429	0.370

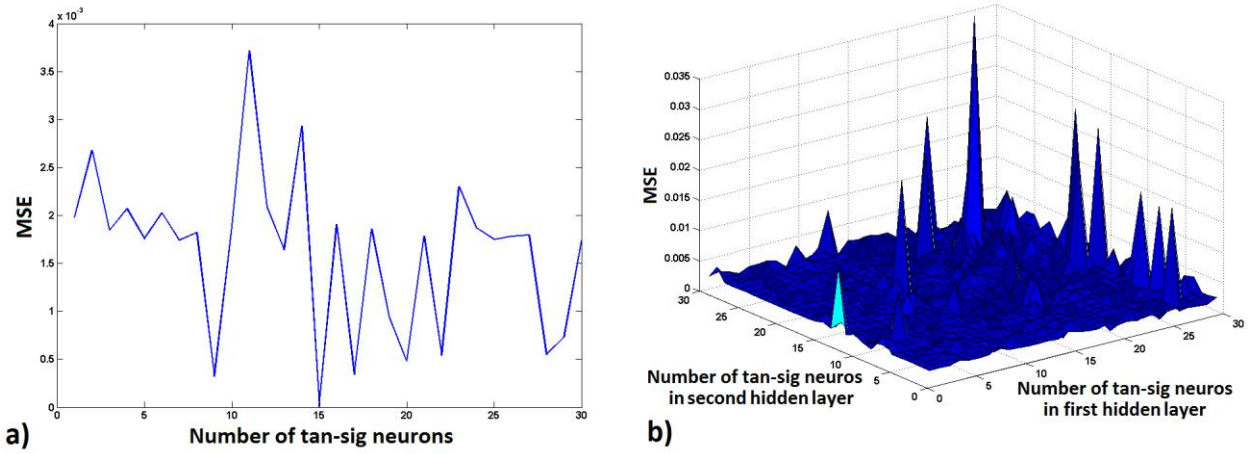

Fig.4. MSE in different networks with various numbers of neurons in hidden layers (One hidden layer (a) and two hidden layers (b))

Table 2. The predicted range of data in microstructure hull and property hull

		max	min	variation
input	porosity volume fraction	0.300	0.533	0.232
	Z growth	0.001	0.991	0.990
	XY growth	0.001	0.991	0.990
	Loading	0.025	0.15	0.125
output	TPB density (L μm^{-2})	0	0.321	0.321
	Contact surface density of particles(L μm^{-1})	0	0.346	0.346
	Gas transport factor	0	0.433	0.433

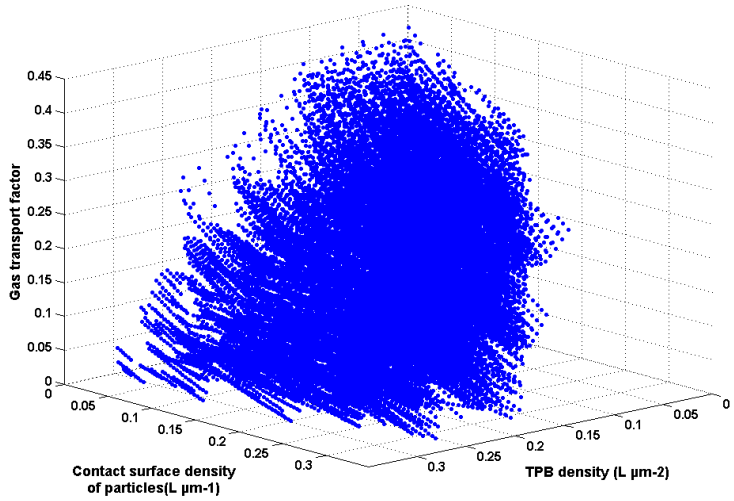

Fig.5. Microstructure property hull, each axis represents one of the desirable properties

Normally, an ideal microstructure have the highest active electrochemical sites (TPB & contact surface density of catalyst particles) and the maximum gas transport factor but the priority of those parameters might be varied depends on the working condition of the electrode. May be a combination of those parameters can be more useful to identify the best microstructures. To clarify the behaviour of those parameters in the property hull, those properties mutually compared when the third parameter is specified with colour as shown in Fig.6.

As shown Fig.6(a), there is not any contradiction between the high level of TPB and contact surface density of particles. But the highest amount of gas diffusivity identified only in the microstructures with lower level of reaction sites. A comparison between gas transport factor and surface density of particles for hypothetical microstructures is shown Fig.6(b). It seems that, increasing the contact surface density has a negative effect on gas transport but the high level of TPB density is feasible in the full range of microstructures. In the other hand, as illustrated in Fig.6(c), TPB density and gas diffusion into the models are inversely related, although there are a limited number of microstructures with high level of reaction sites and acceptable gas diffusivity.

In addition to discover the upper and lower bounds of feasible properties for specific range of microstructures, it is possible to establish a relationship between the effective geometric properties of microstructure in electrochemical and physical reactions in the fuel cells and constructive variables of realized models (backbone porosity, Axial (Z) and transversal (XY) growth rate of backbone grains and loading). For instance, Fig.7(a) illustrates the variation of gas transport factor against the axial growth rate of backbone grains and particle volumetric loading meanwhile the other parameters (traversal growth rate: 0.1 and porosity: 0.5) are set fixed. It can be observed that TPB density steadily increased by changing the particle

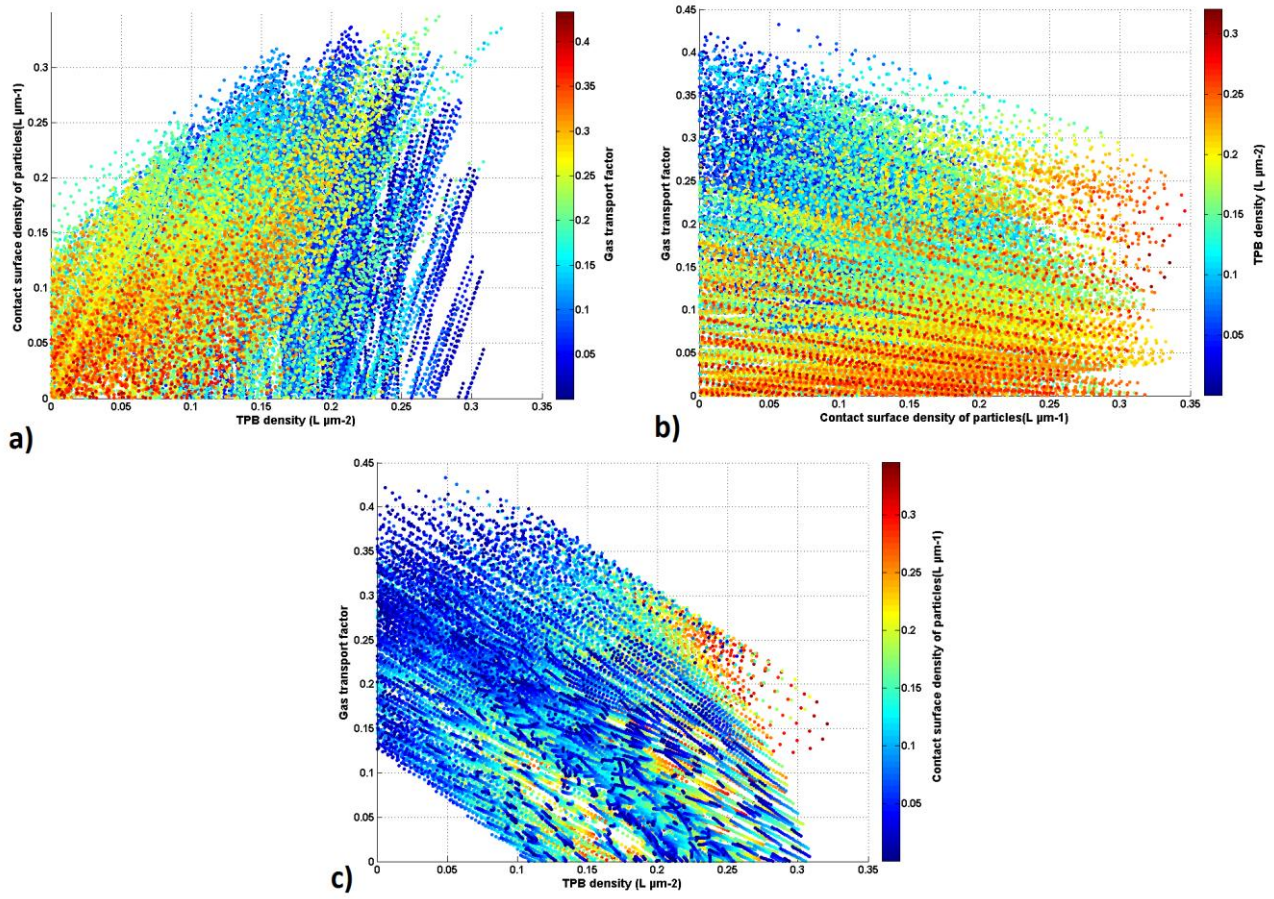

Fig.6.Mutually comparison of microstructures properties in the property hull,
(a) gas transport factor with TPB density
(b) gas transport factor with surface density of particles and
(c) surface density of particles with surface density of particles

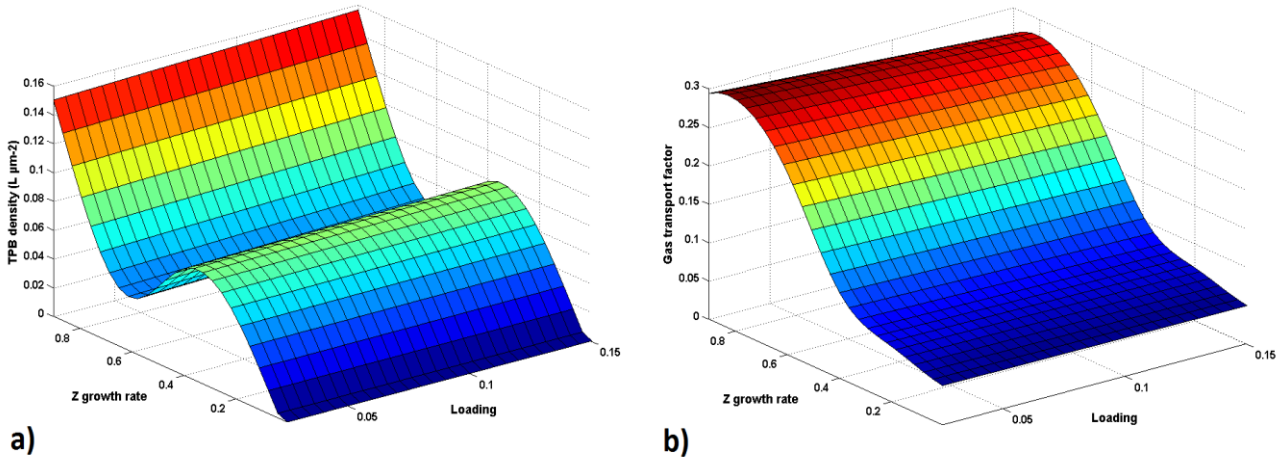

Fig.7.TPB density
(a) and gas transport factor
(b) variation against particle loading and axial growth rate of backbone grains

loading and directional behaviour of backbone grains in Z direction, after a rise and fall, steeply increased. Similarly gas transport factor is plotted over different amount of loadings and axial growth rate of backbone grains in Fig.7(b). when the traversal growth rate: 0.024 and porosity: 0.38 are set fixed. As shown in that figure, being directional normal to the electrolyte apparently increased gas transport and adding particles is limited the diffusivity with a light slope.

To find the optimum virtual models in the hull, a direct search is used to identify those microstructures which are located simultaneously in the upper one third region of the variation range. The microstructural specifications and correlated geometric properties of those 7 models are listed in Table 3.

As reported in that table the best backbone porosity is about 50% in which the axial gain growth rate of scaffold grains is extremely more than the transversal grain growth like needle shape microstructures. The optimum volumetric loading of particles to get the highest level of target properties simultaneously in the microstructures is near to the maximum allowable loading. A realized 3D model based on the average microstructural specifications of optimization process is shown in **Fig. 8**. If the optimization process is concentrated only on the TPB density or other important geometric properties, the constructive specification of model definitely changed based on the target property.

Table 3. the best model parmaters in microstrure and property hull

Microstructure Hull				Property Hull		
backbone porosity	backbone Z growth	backbone XY growth	loading	TPB Density	Surface Density of particles	Gas transport factor
0.492	0.901	0.101	0.103	0.216	0.233	0.285
0.492	0.951	0.101	0.110	0.209	0.265	0.284
0.504	0.951	0.051	0.103	0.213	0.254	0.289
0.516	0.901	0.051	0.129	0.209	0.226	0.282
0.516	0.951	0.051	0.123	0.210	0.280	0.290
0.516	0.951	0.051	0.129	0.218	0.292	0.282
0.528	0.951	0.001	0.129	0.215	0.240	0.282

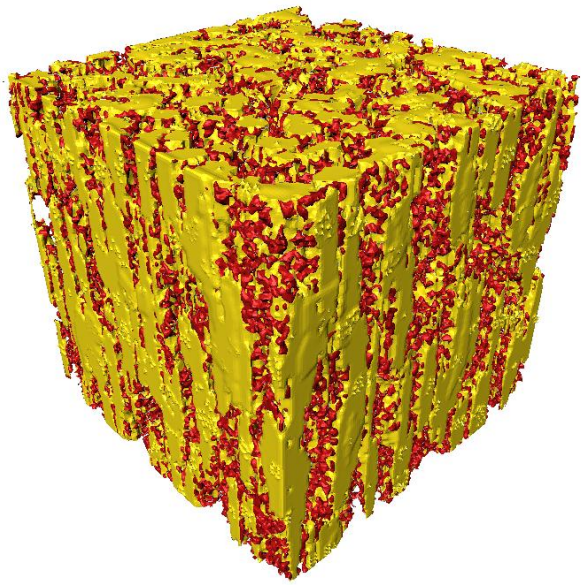

Fig. 8.the 3D-Realized model of optimum microstructure

5.Conclusions

The interactions of backbone geometric anisotropy and the loading of elecrocatalyst particles are investigated via evaluation of microstructural properties in realized voxelized models. To create a general model, at first a series of different directional scaffolds are statistically generated and fully characterized geometrically. Then different amounts of particles are randomly added on the surface of scaffolds as single voxels and a geometric investigation is performed to detect the density of electrochemical active sites (TPB and active surface of particles) and gas transport capability. Those properties are extracted directly from mathematical or 3D realized models. These set of data are used to train a number of feed forward neural networks with one or two hidden layer and various neuron numbers. The best fit model is used to create a property hull of feasible microstructures based on the allowable structural variables like porosity, backbone grain geometric anisotropy and volumetric loading of particles.

The results showed that, directional scaffolds can enhance the TPB density depends on the loading and backbone porosity also the Active surface density of deposited particle is affected by the anisotropy in the backbones. The gas transport factor is strongly affected in directional microstructures in comparison with traditional scaffolds. The property hull is shown the maximum feasible limitations for electrochemical sites also the gas diffusivity and their sensitivity to microstructural geometric parameters. The characteristics of models is shown that there is not any contradiction between the high level of TPB and contact surface density of particles, but the highest amount of gas diffusivity can be found in the microstructures with lower level of reaction sites. Also increasing the contact surface density has a negative effect on gas transport but the high level of TPB density is feasible in the full range of microstructures. I the other hand, TPB density and gas diffusion into the models are inversely related, although there are a limited number of microstructures with high level of reaction sites and acceptable gas diffusivity.

Using a direct search method a list of microstructures with the highest level of reaction sites and gas transport factor are extracted from the property hull. The correlated microstructural identification of those models is shown that the best backbone porosity is about 50%. The axial growth rate of scaffold grains is extremely more than the transversal grain growth like needle shape microstructures. Those parameters guarantee the suitable gas diffusivity in the electrodes. Also the optimum volumetric loading of particles is found near to the maximum allowable loading and the microstructures are not over loaded by the electrocatalyst parties with our assumptions. Generally, if the infiltrated backbones are considered directional, normal to the electrolyte, more electrochemical reaction sites are available in addition to better gas diffusivity.

Eventually, finding the optimal microstructural geometric properties in backbone and deposited particles is a complicated task and strongly associated with most effective electrochemical mechanisms which are determined by the intrinsic property of materials and the working condition of the energy conversion devices. If these kind of modelling approaches are combined with enough experimental data and manufacturing process techniques like 3D printing of additive manufacturing methods, the maximum performance and durability in infiltrated SOFC electrodes can be reached.

6.Acknowledgment

The authors would like to acknowledge the funding for this Project from The Iran National Science Foundation (INSF).

References

[1] Minh N.Q., Takahashi T., Science and Technology of Ceramic Fuel Cells (1995) Elsevier.

[2] Steele B.C., Heinzel A., Materials for Fuel-Cell Technologies, Nature (2001) 414(6861): 345-52.

[3] Minh N.Q., Ceramic Fuel Cells, Journal of the American Ceramic Society (1993) 76(3): 563-588.

[4] Brown M., Primdahl S., Mogensen M., Structure/Performance Relations for Ni/Yttria-Stabilized Zirconia Anodes for Solid Oxide Fuel Cells, Journal of the Electrochemical Society, (2000)147(2):475-85.

[5] Smith J., Chen A., Gostovic D., Hickey D., Kundinger D., Duncan K., Evaluation of the Relationship between Cathode Microstructure and Electrochemical Behavior for SOFCs, Solid State Ionics, (2009)180(1):90-8.

[6] Kishimoto M., Lomberg M., Ruiz-Trejo

E., Brandon N.P., Enhanced Triple-Phase Boundary Density in Infiltrated Electrodes for Solid Oxide Fuel Cells Demonstrated by High-Resolution Tomography, Journal of Power Sources, (2014)266:291-5.

[7] Ni M., Zhao T.S., Solid Oxide Fuel Cells, Royal Society of Chemistry (2013).

[8] Shearing P., Brett D., Brandon N., Towards Intelligent Engineering of SOFC Electrodes, A Review of Advanced Microstructural Characterisation Techniques, International Materials Reviews (2010)55(6): 347-363.

[9] Jiang S.P., Nanoscale and Nano-Structured Electrodes of Solid Oxide Fuel Cells by Infiltration, Advances and Challenges, International Journal of Hydrogen Energy (2012) 37(1): 449-470.

[10] Vohs J.M., Gorte R.J., High-Performance SOFC Cathodes Prepared by Infiltration. Advanced Materials (2009) 21(9): 943-956.

[11] Sarikaya A., Petrovsky V., Dogan F., Development of the Anode Pore Structure and its Effects on the Performance of Solid Oxide Fuel Cells, International Journal of Hydrogen Energy (2013) 38(24): 10081-10091.

[12] Othman M.H.D., Droushiotis N., Wu Z., Kelsall G., Li K., High-Performance, Anode-Supported, Microtubular SOFC Prepared from Single-Step-Fabricated, Dual-Layer Hollow Fibers. Advanced Materials (2011) 23(21): 2480-2483.

[13] Cable T.L., Setlock J.A., Farmer S.C., Eckel A.J., Regenerative Performance of the NASA Symmetrical Solid Oxide Fuel Cell Design, International Journal of Applied Ceramic Technology (2011) 8(1): 1-12.

[14] Gannon P., Sofie S., Deibert M., Smith R., Gorokhovsky V., Thin Film YSZ Coatings on Functionally Graded Freeze Cast NiO/YSZ SOFC Anode Supports, Journal of Applied Electrochemistry (2009)39(4): 497-502.

[15] Chen Y., Bunch J., Li T., Mao Z., Chen F., Novel Functionally Graded Acicular Electrode for Solid Oxide Cells Fabricated by the Freeze-Tape-Casting Process, Journal of Power Sources (2012)213: 93-99.

[16] Chen Y., Zhang Y., Baker J., Majumdar P., Yang Z., Han M., Hierarchically Oriented Macroporous Anode-Supported Solid Oxide Fuel Cell with thin Ceria Electrolyte Film, ACS Applied Materials & Interfaces (2014) 6(7): 5130-5136.

[17] Sofie S.W., Fabrication of Functionally Graded and Aligned Porosity in Thin Ceramic Substrates With the Novel Freeze–Tape-Casting Process. Journal of the American Ceramic Society (2007) 90(7): 2024-2031.

[18] Hen Y., Liu Q., Yang Z., Chen F., Han M., High Performance Low Temperature Solid Oxide Fuel Cells with Novel Electrode Architecture, RSC Advances (2012) 2(32): 12118-12121.

[19] Chen Y., Lin Y., Zhang Y., Wang S., Su D., Yang Z., Low Temperature Solid Oxide Fuel Cells with Hierarchically Porous Cathode Nano-Network, Nano Energy (2014)8: 25-33.

[20] Chen Y., Zhang Y., Lin Y., Yang Z., Su D., Han M., Direct-Methane Solid Oxide Fuel Cells with Hierarchically Porous Ni-Based Anode Deposited with Nanocatalyst layer, Nano Energy (2014) 10: 1-9.

[21] Torabi A., Hanifi A.R., Etsell T.H., Sarkar P., Effects of Porous Support Microstructure on Performance of Infiltrated Electrodes in Solid Oxide Fuel Cells, Journal of the Electrochemical Society (2011)159(2): B201-B210.

[22] Cassidy M., Doherty D.J., Yue X., Irvine J.T., Development of Tailored Porous Microstructures for Infiltrated Catalyst Electrodes by Aqueous Tape Casting Methods. ECS Transactions (2015) 68(1): 2047-2056.

[23] Zhang Y., Sun Q., Xia C., Ni M., Geometric Properties of Nanostructured Solid oxide Fuel Cell Electrodes, Journal of The Electrochemical Society (2013)160(3): F278-F289.

[24]Zhang Y., Ni M., Xia C., Microstructural insights into dual-phase infiltrated solid oxide fuel cell electrodes. Journal of The Electrochemical Society (2013)160(8): F834-F839.

[25] Bertei A., Pharoah J.G., Gawel D.A., Nicolella C., Microstructural Modeling and Effective Properties of Infiltrated SOFC Electrodes, ECS Transactions (2013)57(1): 2527-2536.

[26] Synodis M.J., Porter C.L., Vo N.M., Reszka A.J., Gross M.D., Snyder R.C., A Model to Predict Percolation Threshold and Effective Conductivity of Infiltrated Electrodes for Solid Oxide Fuel Cells. Journal of The Electrochemical Society (2013)160(11): F1216-F1224.

[27]Hardjo E.F., Monder D.S., Karan K., An Effective Property Model for Infiltrated Electrodes in Solid Oxide Fuel Cells. Journal of The Electrochemical Society (2014)161(1): F83-F93.

[28]Reszka A.J., Snyder R.C., Gross M.D., Insights into the Design of SOFC nfiltrated Electrodes with Optimized Active TPB Density via Mechanistic Modeling. Journal of The Electrochemical Society (2014)161(12): F1176-F1183.

[29] Kishimoto M., Lomberg M., Ruiz-Trejo E., Brandon N.P., Towards the Microstructural Optimization of SOFC Electrodes Using Nano Particle Infiltration. ECS Transactions (2014) 64(2): 93-102.

[30] Jemeı S., Hissel D., Péra M.C., Kauffmann J.M., On-Board Fuel Cell Power Supply Modeling on the Basis of Neural Network Methodology, Journal of Power Sources (2003)124(2): 479-486.

[31]Ou S., Achenie L.E., A hybrid neural network model for PEM fuel cells. Journal of Power Sources (2005)140(2): 319-330.

[32] Hagan M.T., Demuth H.B., Beale M.H., De Jesús O., Neural Network Design, PWS Publishing Company Boston(1996) 20.

[33] Marra D., Sorrentino M., Pianese C., Iwanschitz B., A Neural Network Estimator of Solid Oxide Fuel Cell Performance for on-Field Diagnostics and Prognostics Applications, Journal of Power Sources (2013)241: 320-329.

[34]Bozorgmehri S., Hamedi M., Modeling and Optimization of Anode-Supported Solid Oxide Fuel Cells on Cell Parameters via Artificial Neural Network and Genetic Algorithm. Fuel Cells (2012) 12(1): 11-23.

[35] Tafazoli M., Shakeri M., Baniassadi M., Babaei A., Geometric Modeling of Infiltrated Solid Oxide Fuel Cell Electrodes with Directional Backbones, Fuel Cells (2017)17(1):67-74.

[36] Baniassadi M., Ahzi S., Garmestani H., Ruch D., Remond Y., New Approximate Solution for N-Point Correlation Functions for Heterogeneous Materials, Journal of the Mechanics and Physics of Solids (2012)60(1): 104-119.

[37] Baniassadi M., Garmestani H., Li D., Ahzi S., Khaleel M., Sun X., Three-Phase Solid Oxide Fuel Cell Anode Microstructure Realization using Two-Point Correlation Functions, Acta Materialia (2011)59(1): 30-43.

[38] Rüger B., Joos J., Weber A., Carraro T., Ivers-Tiffée E., 3D Electrode Microstructure Reconstruction and Modelling, ECS Transactions (2009)25(2): 1211-1220.

[39] Joos J., Rüger B., Carraro T., Weber A., Ivers-Tiffée E., Electrode Reconstruction by FIB/SEM and Microstructure Modeling, ECS Transactions (2010)28(11): 81-91.

[40]Cai Q., Adjiman C.S., Brandon N.P., Modelling the 3D microstructure and performance of solid oxide fuel cell electrodes: computational parameters. Electrochimica Acta (2011)56(16): 5804-5814.

[41]Jiang Z., C. Xia, Chen F., Nano-Structured Composite Cathodes for intermediate-temperature solid oxide fuel cells via an infiltration/impregnation technique. Electrochimica Acta (2010) 55(11): 3595-3605.

[42]Adler S.B., Lane J., Steele B., Electrode kinetics of porous mixed-conducting oxygen electrodes. Journal of the Electrochemical Society (1996)143(11): 3554-3564.

[43]Babaei A., Jiang S.P., Li J., Electrocatalytic promotion of palladium nanoparticles on hydrogen oxidation on Ni/GDC anodes of SOFCs via spillover. Journal of the Electrochemical Society (2009)156(9): B1022-B1029.

[44]Janardhanan V.M., Heuveline V., Deutschmann O., Three-phase boundary length in solid-oxide fuel cells: A mathematical model. Journal of Power Sources (2008)178(1): 368-372.

[45] Kishimoto M., Lomberg M., Ruiz-Trejo E., Brandon N.P.,Towards the Design-Led Optimization of Solid Oxide Fuel Cell Electrodes. in ECS Conference on Electrochemical Energy Conversion & Storage with SOFC-XIV (2015).

[46]Cronin J.S., Three-Dimensional Structure Combined with Electrochemical Performance Analysis for Solid Oxide Fuel Cell Electrodes (2012).

[47] Shikazono N., Kanno D., Matsuzaki K., Teshima H., Sumino S., Kasagi N., Numerical Assessment of SOFC Anode Polarization Based on Three-Dimensional Model Microstructure Reconstructed from FIB-SEM Images, Journal of The Electrochemical Society (2010) 157(5): B665-B672.

[48]He W., Lv W., Dickerson J., Gas transport in solid oxide fuel cells (2014) Springer.

[49] Fullwood D.T., Niezgoda S.R., Adams B.L., Kalidindi S.R., Microstructure Sensitive Design for Performance Optimization. Progress in Materials Science (2010)55(6): 477-562.

[50]Adams B.L., Kalidindi S., Fullwood D.T., Microstructure-Sensitive Design for Performance Optimization,Butterworth-Heinemann (2013).